Cellular Physiology and Biochemistry

Cell Physiol Biochem 2017;44:172-184
DOI: 10.1159/000484625
Published online: November 07, 2017
Accepted: October 14, 2017

Original Paper

Kinetic Aspects of Verapamil Binding (On-Rate) on Wild-Type and Six *h*K_v1.3 Mutant Channels

Ann-Kathrin Diesch Stephan Grissmer

Institute of Applied Physiology, Ulm University, Ulm, Germany

Key Words
Potassium channel • K_v1.3 channel • Verapamil • Open channel block • Electrophysiology • Patch-clamp

Abstract
Background/Aims: The human-voltage gated K_v1.3 channel (*h*K_v1.3) is expressed in T- and B lymphocytes. Verapamil is able to block *h*K_v1.3 channels. We characterized the effect of verapamil on currents through *h*K_v1.3 channels paying special attention to the on-rate (k_{on}) of verapamil. By comparing on-rates obtained in wild-type (wt) and mutant channels a binding pocket for verapamil and impacts of different amino acid residues should be investigated. ***Methods:*** Using the whole-cell patch clamp technique the action of verapamil on currents through wild-type and six *h*K_v1.3 mutant channels in the open state was investigated by measuring the time course of the open channel block in order to calculate k_{on} of verapamil. ***Results:*** The on-rate of verapamil to block current through *h*K_v1.3_T419C mutant channels is similar to that obtained for *h*K_v1.3_wt channels whereas the on-rate of verapamil to block currents through *h*K_v1.3_L417C and *h*K_v1.3_L418C mutant channels was ~ 3 times slower compared to in wt channels. The on-rate of verapamil to block currents through *h*K_v1.3_L346C and the double mutant *h*K_v1.3_L346C_L418C channel was ~ 2 times slower compared to that obtained in the wt channel. The *h*K_v1.3_I420C mutant channel reduced the on-rate of verapamil to block currents ~ 6 fold. ***Conclusions:*** We conclude that position 420 in *h*K_v1.3 channels maximally interferes with verapamil reaching its binding site to block the channel. Positions 417 and 418 in *h*K_v1.3 channels partially hinder verapamil reaching its binding site to block the channel whereas position 419 may not interfere with verapamil at all. Mutant *h*K_v1.3_L346C and *h*K_v1.3_L346C_L418C mutant channels might indirectly influence the ability of verapamil reaching its binding site to block current.

Introduction

Voltage-gated potassium channels in human T lymphocytes [4] are required for proper T-cell function. Blocking these channels that were later identified to be K_v1.3 channels [1],

Stephan Grissmer

Ulm University, Institute of Applied Physiology
Albert-Einstein-Allee 11, 89081 Ulm (Germany)
Tel. +49 731 500 23253, Fax +49 731 500 36202, E-Mail stephan.grissmer@uni-ulm.de

with known potassium channel blockers like tetraethylammonium would lead to a reduction in T lymphocyte activation measured by radio-active labeled thymidine incorporation after activation of T lymphocytes by phytohaemagglutinin (PHA). This reduction in the immune response was also observed in the presence of verapamil [2], a known blocker of voltage-gated calcium channels, however, voltage-gated calcium channels have not been detected in human T lymphocytes and K_v1.3 channels in T lymphocytes were sensitive to block by verapamil. The K_v1.3 channel (*h*K_v1.3) is a family member of the *Shaker* subfamily of voltage-gated potassium channels. Four identical subunits form the functional channel. Each subunit consists of six transmembrane α-helices S1-S6. The S1-S4 segments provide the voltage sensor, which is responsible for the voltage-dependent control of the pore, whereas the central pore is formed by S5 and S6 [3, 4] through which potassium ions can pass the channel. Human K_v1.3 channels undergo characteristic voltage-dependent structural changes and electrophysiological experiments enable us to distinguish three different functional states [5]. At hyperpolarized potentials the channels do not conduct ions (closed state, C). Depolarization leads to structural rearrangements at the intracellular gate opening the pore and allowing potassium ions to pass the channel across the membrane (open state, O). Keeping the membrane depolarized *h*K_v1.3 potassium channels enter another non-conducting state named C-type inactivated state (I). The inactivation decreases the current flow through the channel during prolonged depolarization which is recognizable by a slow decay in current. This inactivated state is typical for *h*K_v1.3 channels [6]. Previous studies using verapamil in our laboratory showed that one presumed binding site to block the channel is residue A413. To identify this residue important for verapamil binding, several amino acids had been substituted and the equilibrium dissociation constant in the mutant channels was subsequently determined. The mutation of alanine at position 413 to cysteine decreased the affinity of verapamil to block current by approximately 100-fold [7]. In an attempt to get more information about the channel structure and the amino acids in the channel that might interfere with verapamil to reach its binding site, we introduced cysteines and examined in this study the on-rate constant (k_{on}) of verapamil reaching its binding site in the open state of the channel. We mutated residues V417C, L418C, T419C, I420C, L346C and L346C/L418C because some of these residues had been described to interfere with verapamil's ability to block current while the other amino acid substitutions where in close proximity to the presumed binding pocket of verapamil. From the change in current decay during depolarizations in the absence and presence of verapamil we determined the time course of verapamil (τ_{on}) to reduce the current and calculated k_{on}. Figure 1B shows a section of the relevant primary sequence of the S5 and S6 segments of the *h*K_v1.3 channel. Segment S1-S4 are not shown in the figure. We colored all those amino acids - consistently to the colors used in the three-dimensional model - which were mutated to cysteines and therefore are of particular interest for our experiments.

Materials and Methods

Cells

The COS-7 cell line was obtained from the Deutsche Sammlung von Mikroorganismen und Zellkulturen GmbH (DSMZ, Braunschweig, Germany, Cat.No.ACC 60). These cells were cultured in Dulbecco's modified Eagle's medium (DMEM) with 4.5 g_*L^{-1} glucose (Invitrogen, Carlsbad, CA, USA, Cat. No. 41966) containing 10 % fetal bovine serum (Thermo Fisher Scientific, Bonn, Germany, Cat. No. CH30160.02/03). All cells were kept in a humidified incubator at 37°C and 5 % CO_2.

Electrophysiology

All experiments were performed at room temperature (18-22°C) using the whole-cell recording mode of the patch-clamp technique [8]. Cells measured were kept in external bath solution containing in mM: 160 NaCl, 4.5 KCl, 2 $CaCl_2$, 1 $MgCl_2$, 5 HEPES and was adjusted to pH 7.4 with NaOH. The internal pipette solution contained in mM: 155 KF, 10 K-EGTA, 10 HEPES and 1 $MgCl_2$ was adjusted to pH 7.2 with KOH. The osmolarity of both solutions was 290–320 mOsm. The pipettes were pulled from glass capillaries (Science

Product, Hofheim, Germany) in three stages and finally fire polished to resistances of 2-5 MΩ. Currents were acquired using a HEKA EPC9 patch-clamp amplifier (HEKA Elektronik, Lambrecht, Germany) controlled by the stimulation and acquisition software PatchMaster v2x73.4 (HEKA Elektronik). Signals were sampled with a frequency of 1-5 kHz. Patchmaster provides the calculation and subtraction of capacitive and leak currents. A series resistance compensation of 75 % was used for currents exceeding 2 nA.

Cells were plated into little dishes containing a manual, syringe-driven perfusion system which enables changing of the complete external bath solution within 10-30 s. Cells were held at a potential of -120 mV and the number of experiments for each channel was at least three if not mentioned otherwise. Further data analysis was performed with the analysis function of the software Fitmaster v2x73.4 (HEKA Elektronik), Igor Pro 6 (WaveMetrics, Lake Oswego, Or, USA) and Microsoft ® Office Excel 2007 (Microsoft Corporation, Seattle, USA).

Molecular biology

The $hK_v1.3$ wt plasmid was a generous gift from Prof. Dr. O. Pongs (Institut für Neuronale Signalverarbeitung, Zentrum für Molekulare Neurobiologie, Hamburg, Germany). The pRc/CMV (Invitrogen, Carlsbad, Ca, USA) vector contains the $hK_v1.3$_wt potassium channel gene and a CMV promotor for protein expression in mammalian cells. The $hK_v1.3$_V417C, $hK_v1.3$_L418C, $hK_v1.3$_T419C and $hK_v1.3$_I420C mutants were originally constructed in our laboratory by Dr. Tobias Dreker by introducing the corresponding point mutation in the cloned $hK_v1.3$ gene with the Quick-Change site-directed mutagenesis kit (Stratagene, Amsterdam, Netherlands). The $hK_v1.3$_L346C and $hK_v1.3$_L346C_L418C mutants were created by site directed mutagenesis (Eurofins Genomics GmbH, Ebersberg, Germany). The mutations were confirmed by sequencing. The plasmid DNA was transfected into COS-7 cells using the FuGene 6 transfection reagent (Roche Molecular Biochemicals, Mannheim, Germany). Half a day before transfection, cells were plated into 35 mm culture dishes. COS-7 cells were co-transfected using ~2 µg mutant DNA and ~0.5 µg green fluorescent protein, GFP (eGFP-N1 plasmid DNA; Clontech Laboratories, Inc., Palo Alto, CA, USA). The transfected cells were used for electrophysiological measurements 1-3 days after transfection when sufficient protein was expressed at that time.

Fitting equations

Current decay time constants (τ_{decay}) were obtained by fitting the current traces with a modified Hodgkin-Huxley [9] type n^4j model, given by equation

$$I_{total} = I_{K,max} (1 - e^{-t/\tau n})^4 e^{-t/\tau j}$$

as described earlier [10]. I_{total} is the total current, $I_{K,max}$ is the maximum K^+ current, and τ_n and τ_j are time constants of two processes *n* and *j* which represent, respectively, activation and inactivation parameters.

Kinetic model

The kinetic model was performed using XPPAUT5.41 (Bard Ermentrout's tool XPPAUT5.41, Google "xppaut", free software). The models consider several states for wild-type and mutant channels - the closed state (C), the open state (O), the inactivated state (I) and the open-blocked state (OB) as shown in Fig. 1C. Using the following differential equations, simulated current traces were created:

$$dC_1/dt = - \alpha_1 * C_1$$
$$dC_2/dt = \alpha_1 * C_1 - \alpha_2 * C_2$$
$$dC_3/dt = \alpha_2 * C_2 - \alpha_3 * C_3$$
$$dC_4/dt = \alpha_3 * C_3 - \alpha_4 * C_4$$
$$dO/dt = \alpha_4 * C_4 - h * O - k * O + l * OB$$

where C are the closed states, O is the open state, I is the inactivated state and OB is the open-blocked state; α_1 - α_3 describe the forward transitions between the closed states, α_4 describes the transition from the closed to the open state and β_1 – β_4 are the corresponding backward transitions. *h* describes the transition from the open to the inactivated state during depolarizations and *j* describes the backward transition from the inactivated to the open state during depolarization. *k* describes the transition from the open (O) to the open-blocked state and *l* describes the transition from the open-blocked to the open state. In principle the chemical equation includes both directions, however, during depolarization the transitions from the closed to the open state are mainly forward. In addition, we assumed that inactivation is a unidirectional process because the currents during depolarization decayed to zero as has been shown earlier [11]. Therefore we

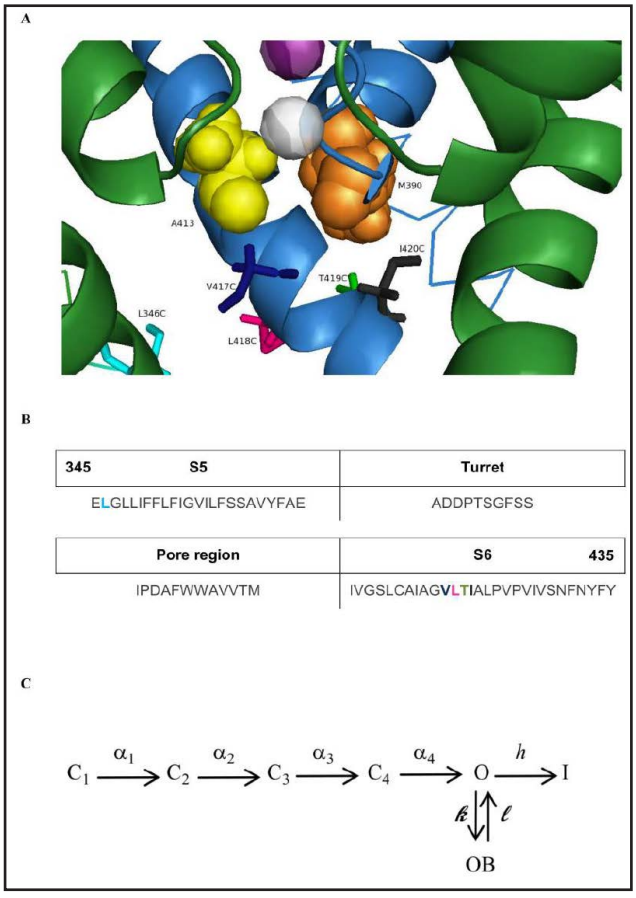

Fig. 1. A, three-dimensional model of the *h*Kv1.3 mutant channel (the K_v1.2 channel [PDB-File: 2A79] was used as a template). Shown is a close-up view. The *h*K_v1.3 mutant channel is composed of four monomers each containing S5, S6 and the P-turn. One subunit is removed. The S5 helices are shown as strands, the P- and S6 helices are shown as smooth helices. For better visualization all side chains of the amino acids were removed except the side chains of the amino acids at positions V417C, L418C, T419C, I420C and L346C. Three subunits are colored green and one subunit is colored blue. Position A413 (yellow), M390 (orange) and K^+ ions (purple) are space-filled. The grey spheres represent non-occupied potassium ion binding sites. Highlighted are amino acid residues that were mutated to cysteines L346C (cyan), V417C (dark-blue), L418C (magenta), T419C (green), I420C (black). B, primary sequence of the S5 and the S6 segment of the *h*K_v1.3 channel. Highlighted are amino acid residues that were mutated to cysteines in my study. L346C (cyan), V417C (dark-blue), L418C (magenta), T419C (green), I420C (black). C, schematic kinetic model of the transitions in *h*Kv1.3 wild-type and mutant channels during depolarization in the presence of verapamil.

did not consider β_{1-4} and *j* to create the simulated current traces using the above described differential equations.

Molecular modeling

The three-dimensional model (3D) of verapamil was obtained as described earlier [12, 13]. As there is no K_v1.3 crystal structure, a template of the K_v1.3 S5/S6 domains was generated using the pdb-file of the crystal structure of the K_v1.2 channel (PDB: 2A79) with a sequence identity over 90% to the K_v 1.3 channel. The K_v1.3 homology model was optimized following the instructions as described earlier [14]. All cysteine mutations were constructed by PyMOL (The PyMOL Molecular Graphics System, Version 1.7 Schrödinger, LLC). Verapamil and the K_v1.3 S5/S6 domains were uploaded together into PyMOL and verapamil was docked manually into the K_v1.3 model structure following instructions from Rossokhin et al. [15].

Materials

Verapamil (Sigma Aldrich Co, Munich, Germany) was prepared as a 100 mM stock solution in DMSO, aliquoted and stored at +4°C. Before using verapamil for experiments the stock solution was diluted in the external bath solution to different final concentrations.

Results

Effect of 100 µM externally applied verapamil on current through hK_v1.3 wt channels

In the first experiment we confirmed the earlier findings that verapamil has an effect on *h*K_v1.3 wild-type channels [5, 7, 16, 17]. Currents through *h*K_v1.3 wild-type channels were first measured in the absence and then in the presence of 100 µM verapamil. Currents

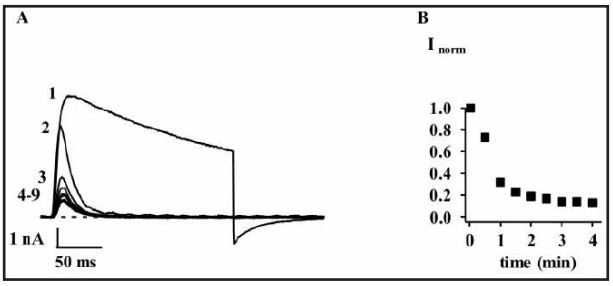

Fig. 2. Effect of extracellularly applied verapamil on currents through wild-type *h*K$_v$1.3 channels. A, Currents were elicited by voltage pulses from a holding potential of -120 to +40 mV for 200 ms every 30 s. Currents were recorded before (trace 1) and after (trace 2-9) external application of 100 µM verapamil. Current traces 7-9 show constant current properties with a steady state peak current. B, Normalized peak currents ($I_{norm} = I_{verapamil}/I_{control}$) obtained from the recorded traces shown in A were plotted against the time.

were elicited by depolarizing pulses from the holding potential of -120 to +40 mV for 200 ms every 30 s in the whole-cell configuration (Fig. 2). In the first trace shown in Fig. 2A cells were kept in an external bath solution containing mainly Na^+ without verapamil. The channels activated fast and current through the channels reached a peak within 20 ms. Following prolonged depolarization, the current in the absence of verapamil decays with a time constant of ~285 ms. This current decay during prolonged depolarization is typical for *h*K$_v$1.3 channels and named C-type inactivation. Right after trace 1 was recorded verapamil was added to the bath solution. The solution exchange was completed before the next traces were recorded (traces 2-9). In principle verapamil has two known effects on currents through *h*K$_v$1.3 channels: i) the time course of the current decay during depolarization accelerates in the presence of verapamil; ii) repetitive pulsing reduces the peak current amplitude until a steady state value is reached. The time course of the current decay during depolarization in the presence of verapamil consists of three separate components: i) the time course of the intrinsic inactivation; ii) the time course of the verapamil block since verapamil does not block the closed state of the channel [5, 18] and iii) the time course of the verapamil unblock (τ_{off}) which is negligible as described later. The acceleration of the time course of the current decay during depolarizations in the presence of verapamill reflects the blocking properties of verapamil. The reduction of the peak current amplitude is caused by an accumulation of verapamil block through a prolonged recovery from inactivation resulting from a blocked-inactivated state [5, 18]. Plotting the normalized peak currents shown in Fig. 2A against the time (Fig. 2B) highlights constant current properties with a steady state peak current after ~6 pulses in the presence of verapamil. To further quantify the effect of verapamil on currents through *h*K$_v$1.3 wild-type channels, we applied different concentrations of verapamil.

Effect of different externally applied verapamil concentrations on current through hK$_v$1.3 wt channels

Figure 3A shows the effect of verapamil on currents through *h*K$_v$1.3 wt channels in the steady state comparable to trace 9 in Fig. 2 at different concentrations of extracellularly applied verapamil. Observed in this experiment was an acceleration of the current decay during depolarization. With higher concentrations of verapamil the time course of the current decay was accelerated. Similar to the experiment shown in Fig. 2, application of different verapamil concentrations also lead to a dose-dependent block of the peak current until a steady state was reached. In Fig. 3B normalized steady state peak current amplitudes from the records shown in Fig. 3A were plotted against the different extracellularly applied verapamil concentrations. The smooth curve was fitted to the measured data points and indicated an equilibrium dissociation constant (K_D) of 18 µM. This value is close to values described earlier using similar protocols [16, 19, 20]. The good agreement of the fit to the data points implies that one verapamil molecule binds reversibly to one *h*K$_v$1.3 channel thereby blocking the current flow through the channel. This steady state value of the dissociation constant K_D depends on the pulse protocol as verapamil blocks in addition to the open state also the inactivated state [18]. K_D can be calculated by the equation

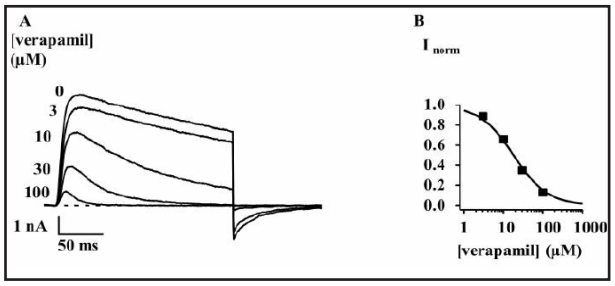

Fig. 3. Effect of extracellularly applied verapamil on steady state currents through wild-type *h*K$_v$1.3 channels. A, Currents were elicited by voltage pulses from a holding potential of -120 to +40 mV for 200 ms every 30 s in the absence and presence of increasing concentrations of verapamil. Shown are steady state currents in different verapamil concentrations as determined and shown in Fig. 2. Numbers on the left side of the traces refer to the applied verapamil concentrations (in μM). B, Dose-response curve for verapamil to block steady state currents through *h*K$_v$1.3 channels. Normalized peak currents ($I_{norm} = I_{verapamil}/I_{control}$) obtained by the indicated drug concentration were plotted against the verapamil concentration. The smooth line represents a fit to the measured data points ($I_{norm} = 1/(1+[VP]/K_D)$ and indicates a K_D value for verapamil of 18 μM.

$K_D = k_{off}/k_{on}$, but the channel closes at hyperpolarization extremely quick. Therefore a rapid exchange of the external solution is required which makes the determination of the time course of the verapamil unblock (τ_{off}) by an experiment very difficult. Therefore we determined in our study the affinity of verapamil by describing the on-rate (k_{on}) constants of *h*K$_v$1.3 channels being blocked in the open state. In the following section we will describe that the change in the time course of the current decay during verapamil application can be used to obtain the on-rate constant k_{on} of verapamil to block the channel.

Current decay time constants (τ_{decay}) lead to on-rate constants (k_{on})

In principle the on-rate constant k_{on} for the reaction of verapamil [VP] with the channel [Ch],

$$[VP] + [Ch] \underset{k_{off}}{\overset{k_{on}}{\rightleftharpoons}} [VP*Ch],$$

can be estimated using the equation $k_{on} = 1/(\tau_{on}*[VP])$ under the assumption that the contribution of the backward reaction is negligible, as suggested by Röbe et al. [18] when no steady-state current during depolarization can be observed. Therefore to determine k_{on}, we need to obtain the time course of verapamil, τ_{on}, to reduce the current. τ_{on} can be determined from the current decay time course (τ_{decay}) during depolarization since this time course consists – in the presence of verapamil – of mainly two separate components as already described above, inactivation and block (the backward transition is very slow). Therefore to determine τ_{on} we first determined the current decay time constants (τ_{decay}) in the presence of different concentrations of verapamil by fitting similar current traces as shown in Fig. 3A with a modified Hodgkin-Huxley model as described in methods (Fig. 4A). Separating the intrinsic inactivation from the effect of blocking the channel by verapamil, τ_{on} was calculated by dividing the time course of the current decay in the presence of different extracellularly applied verapamil concentrations (τ_{decay}) by the time course of the current decay in the presence of control solution without verapamil (τ_j). This approach can be used because during the falling phase of the potassium current, the prevailing transitions are: inactivation with the rate constant *h* and development of block with the rate constant *k* . This leads to the following equation $dO/dt = -h \cdot O - k \cdot O$ that can be solved $O(t) = \exp(-(h+k)\cdot t) = \exp(-h\cdot t)\cdot\exp(-k\cdot t)$ which means that the time course of the current decay in the presence of verapamil is the product of two exponents.

The newly created time course (Fig. 4B) under the above mentioned assumption reflects the time course of verapamil reflects the time course of verapamil to block the open channel (τ_{on}). From τ_{on} we calculated the on-rate (k_{on}) constants of *h*K$_v$1.3 channels being blocked in the open state (Fig. 4C). In contrast to τ_{decay} and τ_{on}, k_{on} does not - as expected - depend on the concentration of verapamil [VP]. Hence for different verapamil concentrations 3, 10, 30

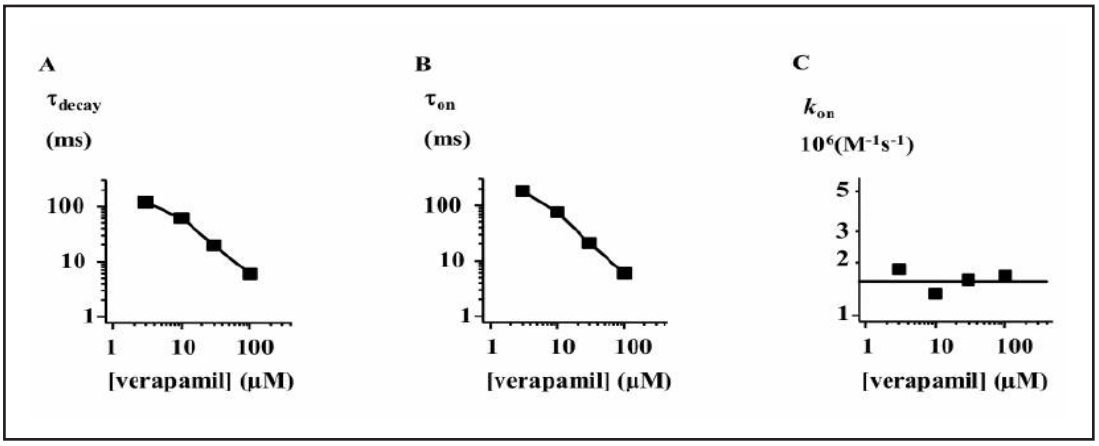

Fig. 4. Estimation of the on-rate constant (k_{on}). A, Current decay time constants (τ_{decay}) of wild-type $hK_v1.3$ currents in the presence of different verapamil concentrations. τ_{decay} was obtained by fitting similar current traces as shown in Fig. 3A with a modified Hodgkin-Huxley [9] type n^4j model as described in methods, given by equation $I_{total} = I_{K,max}(1\text{-}e^{-t/\tau n})^4 e^{-t/\tau j}$as described earlier [10]. τ_{decay} at different concentrations of verapamil were plotted against the externally applied concentration of verapamil. B, Time constants of verapamil (τ_{on}) to block current through wild-type $hK_v1.3$ channels in the presence of different verapamil concentrations. τ_{on} was calculated by dividing the time course of the current decay in the presence of different extracellularly applied verapamil concentrations (τ_{decay}) by the time course of the current decay in the absence of verapamil (τ_j). τ_{on} time constants at different concentrations of verapamil were plotted against the externally applied concentration of verapamil. C, on-rate constants (k_{on}) of verapamil to block current through wild-type $hK_v1.3$ channels in the presence of different verapamil concentrations. k_{on} was calculated using the equation $k_{on} = 1/(\tau_{on}*[VP])$ assuming that the contribution of the backward reaction is negligible. k_{on}constants at different concentrations of verapamil were plotted against the externally applied concentration of verapamil. The line reflects the mean value of $k_{on}$from this experiment of $1.6*10^6$ $M^{-1}s^{-1}$.

and 100 μM we obtained nearly the same values for k_{on} with a mean of $1.6*10^6$ $M^{-1}s^{-1}$(Fig. 4C) similar to values obtained by earlier experiments [5, 7, 16, 18]. This exemplary experiment sets the stage for the following experiments - multiply conducted - with wt and mutant channels.

Since k_{on} can be estimated by the application of a single verapamil concentration, in all following experiments using different mutant $hK_v1.3$ channels, we investigated the effect of verapamil on the time course of current decay during depolarization with 30 μM verapamil.

On-rate constants (k_{on}) of wild-type and $hK_v1.3$ mutant channels in the presence of 30 μM verapamil

In Fig. 5 currents through wild-type, V417C and I420C mutant channels are shown in control solution without verapamil (A-C, traces 1) and in the presence of 30 μM verapamil (A-C, traces 2) which clearly demonstrates different potency of verapamil on current decay. The time constant of current decay of the wild-type channel was decreased by ~8 times to τ_{decay} = 21 ms in the presence of 30 μM verapamil resulting in a k_{on} = $1.39*10^6$ $M^{-1}s^{-1}$ (Fig. 5A). Whereas the time constant of current decay of the V417C mutant channel was decreased ~3 times from τ_j = 222 ms in control solution without verapamil to τ_{decay} = 67 ms in the presence of 30 μM verapamil resulting in a k_{on} = $3.51*10^5$ $M^{-1}s^{-1}$ (Fig. 5B). The I420C mutant channel shows a slower inactivation in the absence of verapamil (τ_j = 753 ms) compared to wt channels as shown in Table 1. The time course of current decay was 7 times faster in the presence of verapamil (τ_{decay} = 107 ms) yielding k_{on} = $2.65*10^5$ $M^{-1}s^{-1}$ (Fig. 5C).

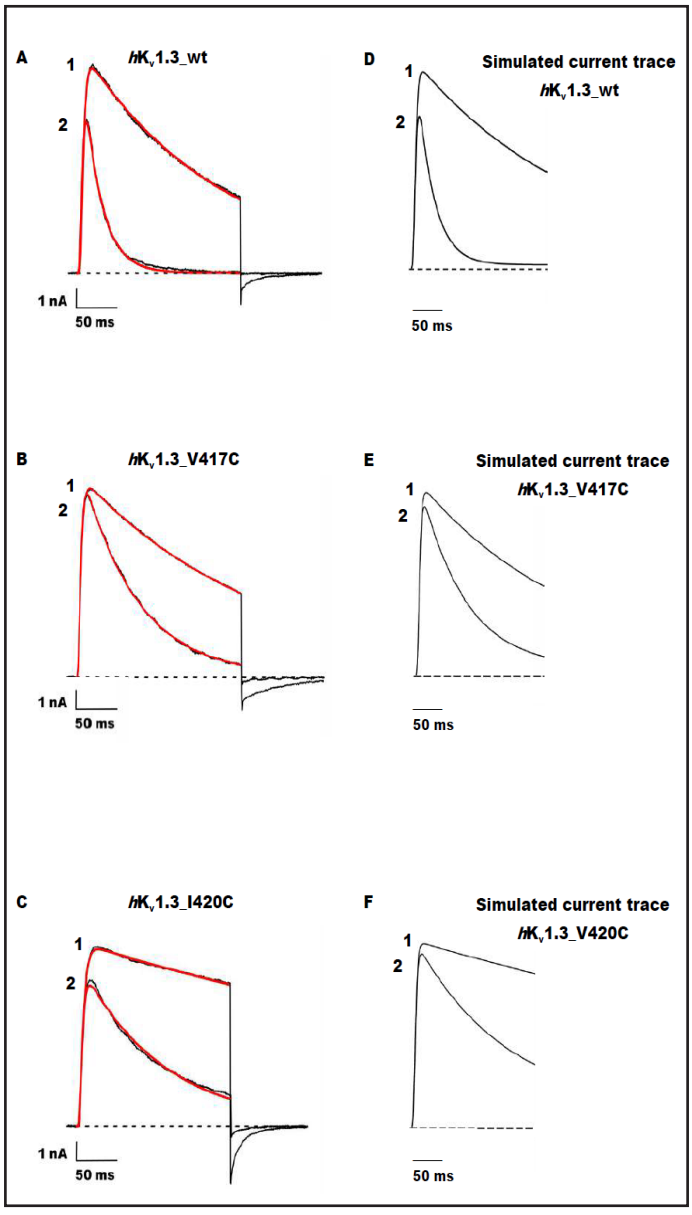

Fig. 5. Effect of the control solution without verapamil (traces 1) and 30 µM extracellularly applied verapamil (traces 2) on currents through A) wild-type *h*K$_v$1.3 channels B) *h*K$_v$1.3_V417C mutant channels C) *h*K$_v$1.3_I420C mutant channels. Currents were elicited by depolarizing pulses from a holding potential of -120 to +40 mV for 200 ms every 30 s. Shown is the first trace in the presence of 30 µM verapamil. The red line is a fit of a modified Hodgkin&Huxley model as described in Fig. 6A to the data points yielding time constant of current decay (τ_{decay}) in the presence of 30 µM verapamil. D-F, simulated current traces using the kinetic diagram described in Methods. All channels occupy state C_1 at the start of the simulation. The parameters used to create the simulated current trace in the presence of 30 µM verapamil were: i) for the *h*K$_v$1.3_ wt channel (D) $\alpha_1 = \alpha_2 = \alpha_3 = \alpha_4 = 0.6$ ms^{-1}, k = 0.037 ms^{-1}; l = 0.0006 ms^{-1}; h=0.004 ms^{-1} ;ii) for the *h*K$_v$1.3_V417C mutant channel (E) $\alpha_1 = \alpha_2 = \alpha_3 = \alpha_4 = 0.6$ ms^{-1}, k = 0.0095 ms^{-1}; l = 0.0006 ms^{-1}; h=0.004 ms^{-1} ;iii) for the *h*K$_v$1.3_I420C mutant channel (F) $\alpha_1 = \alpha_2 = \alpha_3 = \alpha_4 = 0.6$ ms^{-1}, k = 0.0051 ms^{-1}; l = 0.0006 ms^{-1}; h=0.001 ms^{-1} ; in the presence of the control solution without verapamil, the values of k and l were set to zero for each simulation.

Using the kinetic model described in Methods we simulated the currents traces obtained from the measurements shown in Fig. 5A-C in control solution without verapamil (Fig. 5D-F, traces 1) and in the presence of verapamil (Fig. 5D-F, traces 2). Comparing both the experimental and the simulated current traces show that simulations, using the mentioned kinetic model, are in good agreement with the currents experimentally obtained. In addition, the simulated currents verify our above mentioned assumption that the backward reaction is slow when no steady-state current during depolarization occurs. From the simulated current traces we obtained identical values for the off-rate (l) for wild-type channels, V417C and I420C mutant channels implying, that the observed changes in verapamil efficiency to block current through the mutant channel was solely due to changes in k_{on}. This seems to be different from earlier observation by Dreker and Grissmer [7] on the A413C mutation where a steady-state current during 200-ms depolarizations in the presence of verapamil was clearly visible. If one tries to simulate their current trace of the A413C mutant channel

shown in Fig. 2, trace 4 of their paper [7] the trace could only be simulated appropriately if the off-rate of verapamil was raised by a factor of ~100 implying that the backward reaction of verapamil in this case was fast. This increase in the off-rate of verapamil in the A413C mutant channel led us to assume that position A413 is the binding site to block current.

Discussion

In the current study we individually substituted different amino acids in the $hK_v1.3$ channel by cysteines to determine those amino acids in the channel that interact with verapamil. Amino acids at positions V417, L418, T419 and I420 are located consecutively in one turn of the S6 transmembrane α-helix of one subunit of the homotetrameric $hK_v1.3$ channel. We also substituted amino acid L346C in the S5 transmembrane α-helix due to its apparent proximity to position L418. By applying verapamil we examined changes in the on-rate constants (k_{on}) of verapamil to block currents through the open state of the channel by substitutions of amino acids to cysteines in the channel. In principle, the redox status of the cells under investigation could influence the cysteines thereby changing the verapamil binding. However, since we performed our experiments under identical conditions we assume that the redox status did not vary too much from cell to cell. Thus the main focus using cysteines in our study was the change from one amino acid (leucine, valine, threonine, isoleucine) to cysteine rather than from cysteines under a different redox status of the cell. Therefore the aim of this study was to determine which introduced cysteines in the channel can modify verapamil's ability to reach its binding site at position 413 [7] to block current through hKv1.3 channels.

In addition, the above mentioned mutations have not been described in patients and hence we do not know what the impact of those mutants would be on the effect of verapamil *in vivo.*

Table 1. Summary of the effect of six different mutant channels on activation and inactivation in extracellular control solution without verapamil and the effect of extracellularly applied verapamil on currents through wild-type $hK_v1.3$ and six different mutant channels. All values are given as mean ± SD; τ_n, activation time constant in ms in the presence of the control solution without verapamil; τ_j, inactivation time constant in ms in the presence of the control solution without verapamil; τ_{decay}, current decay time constant in ms in the presence of 30 µM verapamil; k_{on}, on-rate constant of verapamil to block current through the channels in $10^6 M^{-1}s^{-1}$; k_{onrel}, relative on-rate constant in % of wild-type. *significant, p<0.01

	wild-type	V417C*	L418C*	T419C	I420C*	L346C*	L346C/L418C*
τ_n	3±0.4 (n=6)	3±0.4 (n=6)	4±0.7 (n=3)	5±0.5 (n=5)	4±0.7 (n=5)	3±0.4 (n=6)	3±1.2 (n=5)
τ_j	187±91 (n=6)	207±38 (n=6)	113±10 (n=3)	282±30 (n=5)	85±164 (n=5)	200±85 (n=6)	111±14 (n=5)
τ_{decay}	26±6 (n=6)	68±13 (n=6)	54±12 (n=3)	23 ± 1 (n=5)	159±40 (n=5)	37±6 (n=6)	38±4 (n=5)
k_{on}	1.1±0.26 (n=6)	0.34±0.07 (n=6)	0.35±0.10 (n=3)	1.30±0.08 (n=5)	0.18±0.03 (n=5)	0.73±0.12 (n=6)	0.58±0.08 (n=5)
k_{onrel}	100	31	32	117	16	66	52

Position 419 in the hK$_v$1.3 mutant channel may not be involved in verapamil reaching its binding site to block current

Regarding the on-rate of the *h*K$_v$1.3_T419C mutant channel which is similar to the on-rate of wild-type channels (Table 1), no significant difference is induced from a change of threonine to a cysteine. Docking verapamil into a homology model of the channel (Fig. 6B-D) shows the possible position of verapamil in the *h*K$_v$1.3 channel and the spatial arrangement of all mutated residues. Since the crystal structure of the *h*K$_v$1.3 channels is not known, we used the crystal structure of the closely related K$_v$1.2 channel (PDB: 2A79) to generate a reasonable structural model. The side chain of amino acid 419 faces away from the inner pore region. As position 419 does not sense the environment of the inner pore, no contact of verapamil occurs during passing from the intracellular side of the channel through the widened bundle crossing (position 423-425; 473- 475 in *Shaker* [21]) when the channel opens, and the on-rate of verapamil to block current through the *h*K$_v$1.3_T419C mutant channel was identical to that obtained in the wild-type *h*K$_v$1.3 channel. This result confirms a previous study by Nikouee et al. [13] who showed that verapamil can prevent MTSEA to modify the cysteine in the *h*K$_v$1.3_T419C mutant channel. It seems that threonine and cysteine only slightly differ in their molecular structure (hydroxyl-group in threonine vs thiolgroup in cysteine) leading to no obvious difference in the on-rate of verapamil.

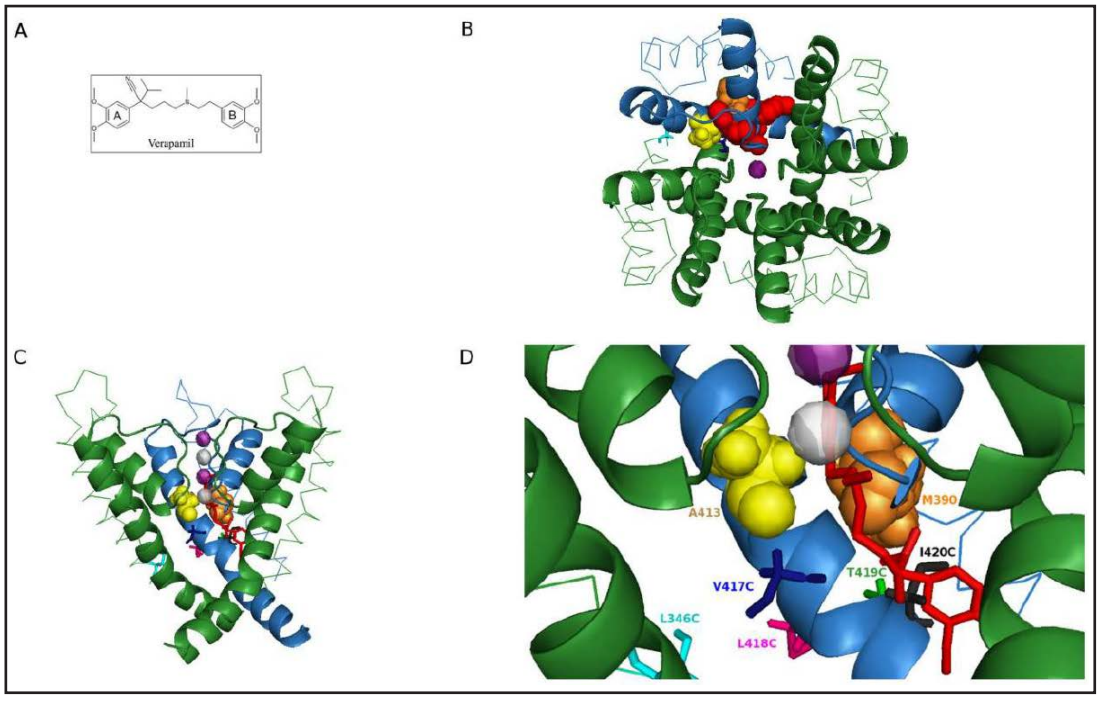

Fig. 6. A, Structural formula of verapamil from Rossokhin et al. [15]. B-D, docking of verapamil (red) into the three-dimensional model of the *h*Kv1.3 mutant channel (the K$_v$1.2 channel [PDB-File: 2A79] was used as a template). Shown are extracellular B, side C and close-up D views. The *h*K$_v$1.3 mutant channel is composed of four monomers each containing S5, S6 and the P-turn. In C and D one subunit is removed. The S5 helices are shown as strands, the P- and S6 helices are shown as smooth helices. For better visualization all side chains of the amino acids were removed except the side chains of the amino acids at positions V417C, L418C, T419C, I420C and L346C. Three subunits are colored green and one subunit is colored blue. Position A413 (yellow), M390 (orange) and K^+ ions (purple) are space-filled. In Fig.6 B verapamil is space-filled. The grey spheres represent non-occupied potassium ion binding sites. Highlighted are amino acid residues that were mutated to cysteines L346C (cyan), V417C (dark-blue), L418C (magenta), T419C (green), I420C (black).

Cysteines at position 417 and 418 in the $hK_v1.3$ channel interfere with verapamil

Extracellular application of verapamil on V417C and L418C mutant channels resulted in a similar reduction of the on-rate constant to about one third compared to $hK_v1.3$_wt channels. This could be a hint that these two residues make it more difficult for verapamil to reach its binding site to block current presumably by obstructing the channel thereby reducing k_{on} and prolonging the time verapamil needs to reach its binding site to block the channel. This may confirm the suggestion that by binding at position A413 [7] verapamil also partially covers position 417 [13]. The latter authors also showed that verapamil cannot protect the cysteine at position 418 from MTSEA modification. Taking together these results indicate that the amino acids at position 417 and 418 can modify verapamil's ability to reach its binding site to block the channel. Once verapamil reaches its binding site to block current (A413), verapamil also partially covers position 417 but not 418. It seems that only position 417 participates in the binding pocket for verapamil.

Position 346 in the $hK_v1.3$ channel might indirectly influence verapamil's ability to reach its binding site to block current

The crystal structure showed that the amino acid residue at position 346 in the S5 segment of the $hK_v1.3$ channel is in close proximity to position 418 of the neighboring subunit (~7Å). Thus we wanted to examine whether position 346 can also modify verapamil's ability to block current. The relative on-rate constant was reduced by about one third in the L346C single mutant channels compared to wild-type channels. The $hK_v1.3$_L346C_L418C double mutant also showed a decline in the on-rate constant by 48 %. With reference to the on-rate of verapamil, both the single and the double mutant channel seem to be involved in verapamil binding. However taking a closer look at position L346 in the channel, the amino acid is located in S5 which is not lining the inner pore and seems to be far away from the verapamil binding site to block current. Therefore we assume that the mutation of position 346 from leucine to cysteine is changing the overall structural conformation of the channel thereby indirectly influencing the verapamil on-rate constant. An allosteric effect of the mutation on the overall structure of the channel itself could be an argument for all mutations examined in this study. But it seems to be more evident for position 346 because of the greater distance to the inner pore region.

Position 420 in the $hK_v1.3$ channel has a major effect on the on-rate of verapamil

Compared to all other examined mutants, maximum effect on the on-rate constant of verapamil had a mutation from isoleucine to cysteine at position 420. k_{on} was reduced to about one sixth compared to wild-type channels. Figure 6 shows that by binding at position 413, verapamil gets into close contact to position 420. Ring A of verapamil (Fig. 6A) seems to stick between the side chain of position 420. Due to the similar structure of the aromatic rings, a possible explanation for the decreased on-rate constant might be that Ring B of verapamil first passes and interferes with position 420 before it can reach its binding site to block current. This is an indication, that position 420 is also a presumed binding position thereby decreasing the blocking properties of verapamil. For a large molecule like verapamil the existence of more than one binding site is reasonable, supporting the proposal that position 420 is a crucial component of the binding site to block the channel and participates in the binding pocket for verapamil.

Docking of verapamil in the $hK_v1.3$ mutant channel

According to the lowest-energy model of [15] we modeled the presumed position of verapamil in $hK_v1.3$ channels (Fig. 6, B-D). Locating verapamil's *para*-oxygen in ring B in proximity to position 413, it was placed at a distance of 6 Å from the β-carbon of position 413. The hydrogen atom of the ammonium group covalently binds to the backbone carbonyl of position 391. The *meta*- and *para*-methoxy groups of ring B are able to penetrate the intrasubunit niche reaching the side chains of position 390 and 413. Using this model, the *metha*-methoxy group in ring B approaches position 390 which is also consistent with a

former study. Rauer and Grissmer [22] proposed position 390 being a binding site to block the channel, as the affinity for verapamil was decreased about 6 fold. In this configuration the distance of ring A to the cysteine at position 420 was approximately 1 Å and to position 417 3 Å. This differential proximity could also explain the change in verapamil's k_{on} with mutations at these positions observed in our experiments.

Conclusion

Considering all on-rate constants of different mutants in this study (Table 1) and the homology model of the hK$_v$1.3 channel, respectively, we gained insight into the ability of verapamil reaching its binding site to block current after passing through hK$_v$1.3 channels in the open state. Verapamil applied extracellularly passes through the membrane in neutral form [5] and reaches the presumed binding position A413 from the intracellular side [16] after the bundle crossing positions (position 423-425) widen [5, 17]. Amino acids 417-420 constitute one turn of the S6 transmembrane α-helix. Position V417, the first amino acid of the turn and position I420 the terminal amino acid of the turn, face towards the center of the inner pore. Amino acids L418 and T419 face away from the center of the inner pore towards the outside of the helical turn. After verapamil enters the pore of the channel it first passes through the widened bundle crossing then reaches position I420C which already interacts with verapamil and constitutes a verapamil binding position. Both amino acids V417C and L418C extend into the inner pore of the channel. It seems that these two cysteines at the positions partially interfere with verapamil after verapamil passed the constricted opening at position I420 reaching its binding site to block current. T419 is facing away from the center of the inner pore in the open state of the channel. Due to this positioning it does not have an impact on verapamil's ability to reach its binding site to block current. Since position 346 in the S5 segment is not close to the verapamil binding site to block the channel we conclude that a mutation at this position indirectly changed the on-rate constant of verapamil presumably by influencing the arrangement of the α-helices of S5 thereby modulating S6. Additional experiments with verapamil analogues (e.g. anipamil, ronipamil, emopamil) might identify further contact points between the channel and verapamil in an attempt to more clearly define the binding position of verapamil within the channel.

Abbreviations

GFP (green fluorescent protein); VP (verapamil); wt (wild-type).

Acknowlegements

The authors would like to thank Ms Katharina Ruff for her excellent technical assistance. We thank Prof Dr O. Pongs who generously gave us the plasmid for the wild-type hK$_v$1.3 channel; Dr Tobias Dreker who introduced the V417C, L418C, T419C and I420C point mutations in the hK$_v$1.3channel. This work was supported by a grant from the Deutsche Forschungsgemeinschaft to S.G. [Grant 848/17-1].

Disclosure Statement

The authors declare no conflict of interest.

References

1 Grissmer S, Dethlefs B, Wasmuth JJ, Goldin AL, Gutman GA, Cahalan MD, Chandy KG: Expression and chromosomal localization of a lymphocyte K^+ channel gene. Proc Natl Acad Sci U S A 1990;87:9411–9415.
2 Chandy KG, DeCoursey TE, Cahalan MD, McLaughlin C, Gupta S: Voltage-gated potassium channels are required for human T lymphocyte activation. J Exp Med 1984;160:369–385.
3 Long SB, Campbell EB, MacKinnon R: Crystal structure of a mammalian voltage-dependent *Shaker* family K^+ channel. Science 2005;309:897–903.
4 Long SB, Campbell EB, MacKinnon R: Voltage sensor of Kv1.2: structural basis of electromechanical coupling. Science 2005;309:903–908.
5 DeCoursey TE: Mechanism of K^+ channel block by verapamil and related compounds in rat alveolar epithelial cells. J Gen Physiol 1995;106:745–779.
6 DeCoursey TE, Chandy KG, Gupta S, Cahalan MD: Voltage-gated K^+ channels in human T lymphocytes: a role in mitogenesis? Nature 1984;307:465–468.
7 Dreker T, Grissmer S: Investigation of the phenylalkylamine binding site in *h*Kv1.3 (H399T), a mutant with a reduced C-type inactivated state. Mol Pharmacol 2005;68:966–973.
8 Hamill OP, Marty A, Neher E, Sakmann B, Sigworth FJ: Improved patch-clamp techniques for high-resolution current recording from cells and cell-free membrane patches. Pflugers Arch 1981;391:85–100.
9 Hodkin AL Huxley, AF: A quantitative description of membrane current and its application to conduction and excitation in nerve. J Physiol 1952; 117: 500-544.
10 Cahalan MD, Chandy KG, DeCoursey TE, Gupta S: A voltage-gated potassium channel in human T lymphocytes. J Physiol 1985;358:197–237.
11 Grissmer S, Cahalan M: TEA prevents inactivation while blocking open K^+ channels in human T lymphocytes. Biophys J 1989;55:203–206.
12 Schuttelkopf AW, van Aalten, Daan M F: PRODRG: a tool for high-throughput crystallography of protein-ligand complexes. Acta Crystallogr D Struct Biol 2004;60:1355–1363.
13 Nikouee A, Janbein M, Grissmer S: Verapamil- and state-dependent effect of 2-aminoethylmethanethiosulphonate (MTSEA) on *h*Kv1.3 channels. Br J Pharmacol 2012;167:1378–1388.
14 Prütting S, Grissmer S: A novel current pathway parallel to the central pore in a mutant voltage-gated potassium channel. J Biol Chem 2011;286:20031–20042.
15 Rossokhin A, Dreker T, Grissmer S, Zhorov BS: Why does the inner-helix mutation A413C double the stoichiometry of Kv1.3 channel block by emopamil but not by verapamil? Mol Pharmacol 2011;79:681–691.
16 Rauer H, Grissmer S: Evidence for an internal phenylalkylamine action on the voltage-gated potassium channel Kv1.3. Mol Pharmacol 1996;50:1625–34.
17 Jacobs ER, DeCoursey TE: Mechanisms of potassium channel block in rat alveolar epithelial cells. J Pharmacol Exp Ther 1990;255:459–472.
18 Robe RJ, Grissmer S: Block of the lymphocyte K^+ channel *m*Kv1.3 by the phenylalkylamine verapamil: kinetic aspects of block and disruption of accumulation of block by a single point mutation. Br J Pharmacol 2000;131:1275–1284.
19 DeCoursey TE, Chandy KG, Gupta S, Cahalan MD: Voltage-dependent ion channels in T-lymphocytes. J Neuroimmunol 1985;10:71–95.
20 Chandy KG, Gutman GA, Grissmer S: Physiological role, molecular structure and evolutionary relationships of voltage-gated potassium channels in T lymphocytes. Semin Neurosci 1993;5:125–134.
21 Tombola F, Pathak MM, Isacoff EY: How does voltage open an ion channel? Annu Rev Cell Dev Biol 2006;22:23–52.
22 Rauer H, Grissmer S: The effect of deep pore mutations on the action of phenylalkylamines on the Kv1.3 potassium channel. Br J Pharmacol 1999;127:1065–1074.